Polar Science 10 (2016) 564–575

Contents lists available at ScienceDirect

Polar Science

journal homepage: https://www.evise.com/profile/#/JRNL_POLAR/login

Operational high latitude surface irradiance products from polar orbiting satellites

Øystein Godøy

Norwegian Meteorological Institute, Henrik Mohns Plass 1, 0313 Oslo, Norway

ARTICLE INFO

Article history:
Received 1 January 2016
Received in revised form
9 October 2016
Accepted 14 October 2016
Available online 18 October 2016

Keywords:
AVHRR
Shortwave
Longwave
Irradiance
Satellite

ABSTRACT

It remains a challenge to find an adequate approach for operational estimation of surface incoming short- and longwave irradiance at high latitudes using polar orbiting meteorological satellite data. In this presentation validation results at a number of North Atlantic and Arctic Ocean high latitude stations are presented and discussed. The validation results have revealed that although the method works well and normally fulfil the operational requirements, there is room for improvement. A number of issues that can improve the estimates at high latitudes have been identified. These improvements are partly related to improved cloud classification using satellite data and partly related to improved handling of multiple reflections over bright surfaces (snow and sea ice), especially in broken cloud conditions. Furthermore, the availability of validation sites over open ocean and sea ice is a challenge.

1. Introduction

The surface radiation budget is an essential parameter for understanding our biological and physical environments. Over land, surface observations are quite frequent, while such observations are sparse over ocean areas. World Climate Research Programme (WCRP) initiated the Baseline Surface Radiation Network (BSRN, Ohmura et al., 1998), providing high quality in situ measurements for validation of satellite and climate model estimates of the surface radiation budget. In addition to these high quality measurements, a number of measurements of lesser quality also exist. However, these do by no mean cover all areas and are usually most dense over populated areas. Satellite remote sensing provides a mechanism to fill in the spatial gaps between the in situ measurements in order to provide spatially consistent products. These products can be useful for comparison with numerical simulations (especially since the cloud information is more accurate than cloud information from numerical simulations), for usage in biology etc.

The Norwegian Meteorological Institute (METNO) is part of the European Organization for the Exploitation of Meteorological Satellites (EUMETSAT) Satellite Application Facility (SAF) for Ocean and Sea Ice (OSISAF, see http://www.osi-saf.org/). Within this framework METNO is part of the High Latitude (HL) Processing Centre and has developed a system for estimation of the Surface Solar Irradiance (SSI) and Downward Longwave Irradiance (DLI) at the surface using polar orbiting satellites (NOAA and EUMETSAT). Similarly, for low and mid latitudes, Météo-France has developed and implemented algorithms doing the same, but using geostationary satellite information as input. Algorithms and processing is tuned for ocean areas although validation data in such conditions are sparse.

SSI is estimated from single passage AVHRR data. Single passage products are combined into a daily product at 5 km horizontal resolution and on a polar stereographic map projection. Data are presented north of 50°N at present.

This presentation provides details on how the OSISAF SSI and DLI products are generated using AVHRR data as input and how these products can be validated. These products were not included in the validation performed by Ineichen et al. (2009) and are validated using stations that are located further north than that study. The time period being examined is January 2013 through September 2015.

First the method is outlined, then the results are presented and discussed with final comments in the conclusion.

2. Methods and data

2.1. Surface solar irradiance

The solar irradiance at the surface (E) is a function (Eq. (1)) of the solar irradiance at the top of the atmosphere, the clear sky

E-mail address: o.godoy@met.no.

http://dx.doi.org/10.1016/j.polar.2016.10.001

atmospheric transmittance (T_a), and the combined effects of clouds through a cloud factor (T_{cl}) (e.g. Brisson et al., 1994, 1999):

$$E = S'\mu_0 T_a T_{cl}$$
$$S' = \frac{S_0}{\rho^2} \quad (1)$$
$$\mu_0 = \cos\sigma$$

where σ is the solar zenith angle, S_0 is the solar constant (approximately 1367 W/m^2). ρ^2 (Eq. (2)) is a correction factor for the varying distance between the Earth and the Sun. The annual cycle in the extraterrestrial solar irradiance is approximately ±3% about the mean due to a variation in the distance between the Earth and the Sun. This variation can be defined in different ways, but here the specification of Paltridge and Platt (1976) will be used.

$$\rho^2 = \frac{1}{1.00011 + 0.034221\ \cos\theta + 0.001280\ \sin\theta + 0.000719\ \cos 2\theta + 0.000077\ \sin 2\theta} \quad (2)$$

where

$$\rho = \frac{D^{SE}}{\overline{D^{SE}}} \quad \text{and} \quad \theta = \frac{2\pi d_n}{365}$$

D^{SE} is the actual distance between the Sun and the Earth and $\overline{D^{SE}}$ is the mean distance (referring to 1AU). d_n is the day of the year starting at 0 on January 1 and ending at 364 on December 31.

The parametrisation used for clear sky atmospheric transmittance (T_a) in this study (Eq. (3)) is described in Darnell et al. (1988, 1992). It was evaluated in Godøy (2000). This parametrisation is independent of the satellite observation. It includes the effect of absorption in water vapour, ozone, oxygen, and carbon dioxide, as well as scattering by aerosols and Rayleigh scattering. The atmospheric back-scatter of surface reflected rays is parametrized by the surface pressure (p_s) and albedo (A_s):

$$T_a = e^{-\tau}(1 + 0.065 p_s A_s)$$
$$\tau = \tau_0 \left(\frac{1}{\mu_0}\right)^N, \quad where\ N = 1.1 - 2\tau_0$$
$$\tau_0 = \tau_{O3} + \tau_{H2O} + \tau_{O2} + \tau_{CO2} + \tau_R + \tau_a$$
$$\tau_{O3} = 0.038 U_{O3}^{0.44}$$
$$\tau_{H2O} = 0.104 U_{H2O}^{0.3} \quad (3)$$
$$\tau_{O2} = 0.0075 p_s^{.87}$$
$$\tau_{CO2} = 0.0076 p_s^{0.29}$$
$$\tau_R = 0.038 p_s$$
$$\tau_a = 0.007 + 0.009 U_{H2O}$$

In the equations above, τ represents the optical depth due to various absorbers, μ_0 is as before the cosine of the solar zenith angle, p_s is the nominal surface atmospheric pressure in atmospheres and U is the atmospheric load (in cm) of various constituents. The cloud factor (T_{cl}) is a function of the cloud albedo and requires several processing steps to be determined.

1. AVHRR counts are converted to scaled radiance by the approach described by NOAA. This is a reflectance measure for overhead Sun.
2. The scaled radiance is converted to a pseudo bi-directional reflectance by division with the cosine of the solar zenith angle and correction for the distance between the Earth and the Sun (Eq. (2)).
3. Narrowband to broadband correction (Hucek and Jacobowitz, 1995).
4. Anisotropy correction (Manalo-Smith et al., 1998).

The result is a directional independent measure of the cloud albedo. However, it is well known that the visible channels of the AVHRR instrument is subject to degradation with time (e.g. Rao and Chen, 1996, 1999) after satellite launch. The corrections for AVHRR released regularly by NOAA through http://noaasis.noaa.gov/NOAASIS/ml/calibration.html are implemented in the processing when available.

Generally the cloud transmittance is related to the cloud albedo through the relationship (Eq. (4)).

$$a_c + T_c + A_c = 1 \quad (4)$$

where a_c represents cloud absorption, T_c represents cloud transmittance and A_c represents cloud reflection which is interpreted as albedo in this context following the narrowband to broadband and anisotropy corrections. This basically means that what is not transferred through a layer is either reflected by or absorbed in the layer. The main problem for estimation of satellite derived SSI is to determine the effects of clouds on radiation (multiple reflection, transmission, absorption). These processes have to be related to the observed cloud albedo and knowledge of the atmospheric conditions. This method is described in Frouin and Chertock (1992). The first equation (Eq. (5)) below relates the satellite observed albedo (A) to the combined cloud and surface albedo (A'). The second equation (Eq. (6)) describes the cloud absorption as a function of the combined albedo of the cloud and the surface and the surface albedo. By subtracting the surface albedo from the combined albedo, the cloud albedo remains. This is related to the cloud absorption through a cloud absorption factor (m). Originally (Frouin and Chertock, 1992) the relationship depended on a factor α which varied from 0.03 to 0.4, according to cloud liquid water content and the solar zenith angle (increasing zenith and liquid water gives decreasing α). In this implementation, α is replaced by $m\mu_0$. This implies that the dependency of cloud liquid water content is constant while the solar zenith angle dependency is dynamic. However, the combined effect of $m\mu_0$ is confined within the limits specified for α. The third equation (Eq. (7)) represents the cloud factor (T_{cl}), that is the effect of clouds on the irradiance that reach the surface.

$$A = A_{ray} + \frac{T_{dt} A'}{1 - S_a A'} \quad (5)$$

$$a_c = m\mu_0 (A' - A_s) \quad (6)$$

$$T_{cl} = \frac{1 - A' - a_c}{1 - S_a A'} \tag{7}$$

In the equations above A' is the combined cloud and surface albedo, a_c is the cloud absorption, A_s is the surface albedo, and T_{dt} is the Sun-Cloud-Satellite transmittance. A_{ray} represents the contribution of scattering in a clear atmosphere to the observed albedo. No formula is given for A_{ray}, thus the formulation for Rayleigh scattering given by Brisson et al. (1999) was used. $T_{dt}A'(1\text{-}S_aA')^{-1}$ represents the contribution from multiple scattering by the cloud layer (including photons reflected from the surface). S_a is the spherical albedo and accounts for multiple reflection between the surface and the cloud. In this configuration, T_{cl} represents the ratio between the irradiance that reaches the surface and the irradiance that would have reached the surface under cloud free conditions. In other words this is the combined effect of absorption in the cloud and reflection by the cloud (and surface) on the incoming radiation. This ratio depends on the solar zenith angle.

Further description of choices made in the configuration of the SSI processing is provided in Technical Reports (Godøy, 2000; Godøy and Eastwood, 2002a, 2002b, 2002c). A schematic representation of the SSI processing chain is provided in Fig. 1. This shows that the main purpose of the satellite data is to provide a description of the cloud condition.

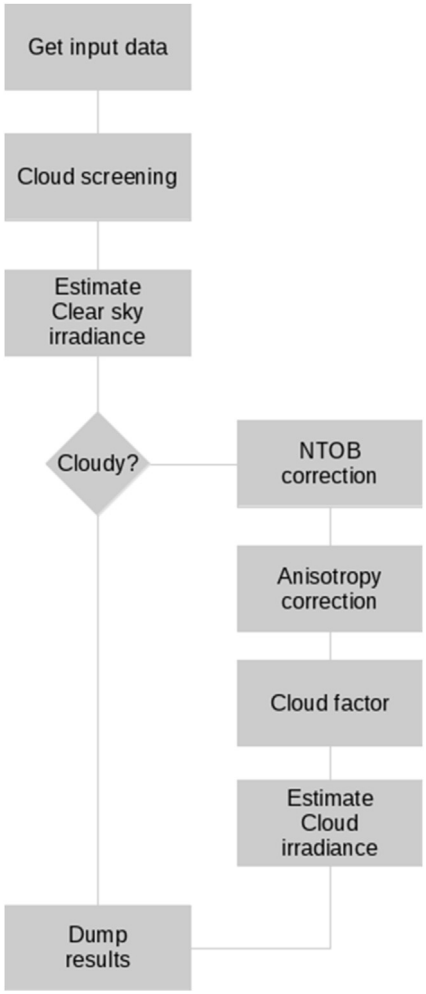

Fig. 1. Schematic representation of the SSI processing chain.

2.2. Downward longwave irradiance

The OSISAF HL algorithm for Downward Longwave Irradiance (DLI) is a bulk parametrisation with extensive use of Numerical Weather Prediction (NWP) model input. The clear sky DLI is estimated using NWP only. In presence of clouds this is corrected by applying the cloud type product (Dybbroe et al., 2005a, 2005b; Karlsson and Dybbroe, 2010), generated by the EUMETSAT SAF on Support to Nowcasting and Very Short Range Forecasting (NWCSAF) Polar Platform System (PPS) software.

According to experience gained developing algorithms for Low and Mid Latitude within the OSISAF (Brisson et al., 2000), a hybrid method was chosen for estimation of DLI. This is a combination of a bulk parametrisation and a satellite derived cloud amount. The basis for the method is briefly described in Godøy (2004) and by the equations below. DLI (Eq. (8)) is estimated using the Stefan-Boltzmann law, a clear sky emissivity (ε_0) and a cloud contribution coefficient (C).

$$L = (\varepsilon_0 + (1 - \varepsilon_0)C)\sigma T_{air}^4 \tag{8}$$

ε_0: clear sky emissicity.C: infrared cloud amount.σ: Stefen- Boltzmann constant $\left(5.6696 \times 10^{-8} \frac{W}{m^2 K^4}\right)$.$T_{air}$: Air temperature (Kelvin).

The cloud contribution is estimated (Eq. (9)) by summarizing individual cloud contribution coefficients and the fractional cloud cover.

$$C = \sum_i (n_i C_i) \tag{9}$$

C_i: contribution coefficient by cloud type i.n_i: fractional cloud cover by cloud type i.

The DLI (L) in Eq. (8) is a sum of the clear sky emitted irradiance (first term), the contribution from cloud (second term), minus the clear sky contribution obscured by clouds.

The main challenge is to determine the method to use for the clear sky emissivity, how to determine the cloud amount and how to actually implement the method in practise.

To estimate the clear sky emissivity (Eq. (10)), the formulation of Prata (1996) is used.

$$\varepsilon_0 = 1 - (1 + \xi)\exp\left[- \sqrt{(1.2 + 3.0\xi)} \right] - 0.05\frac{(p_0 - p)}{(p_0 - 710)}$$
$$p_0 : 1013.25[hPa] \tag{10}$$

Where

$$\xi = c\left(\frac{e_0}{T_{air}}\right) \tag{11}$$

Where e_0 is surface water vapour pressure, $46.5\left[\frac{cm\ K}{hPa}\right]$.

As the method of Prata (1996) needs the surface water vapour pressure (e_0) as input, this is estimated using the product of the saturation water vapour pressure (e_s) and relative humidity (R_h). e_s is estimated using the Goff- Gratch equation (below) (Goff and Gratch, 1946; List, 1984). The two equations below (Eq. (12)) provide the saturation water vapour pressure over plane surfaces of water and ice as a function of the air temperature (T_{air}).

$$\begin{aligned} &If\ \ T_{air} > 273.15\ \ use: \\ &e_s = 10^{(23.8319 - 2948.964/T_{air} - 5.028\ \log_{10}T_{air} - 29810.16\ \exp(-0.0699382T_{air}) + 25.21935\ \exp(-2999.924/T_{air}))} \\ &If\ \ T_{air} < 273.15\ \ use: \\ &e_s = 10^{(2.07023 - 0.00320991T_{air} - 2484.896/T_{air}) + 3.56654\ \log_{10}T_{air}} \end{aligned} \tag{12}$$

Concerning the determination of C_i, at least two different methods can be used. Brisson et al. (2000) showed that cloud contribution coefficients can be estimated using surface pyrgeometer observations according to the equation below.

$$C_i = \frac{\left(L_m - \varepsilon_0 \sigma {T_{air}}^4\right)}{\left((1 - \varepsilon_0)\sigma {T_{air}}^4\right)} \tag{13}$$

L_m: Observed downward longwave irradiance.

Given a classified satellite image a contribution coefficient can be estimated for each cloud type represented in the classified image.

However, Brisson et al. (2000) also presented another method that can be used to infer C. This method (Eq. (14)) is only applicable during daytime and is based upon use of the SSI product.

$$C = 1 - \frac{E}{E_{clr}} \tag{14}$$

where E is the estimated surface solar irradiance (SSI) using AVHRR data, E_{clr} is the clear sky calculated SSI.

In this equation the infrared cloud amount is directly related to the optical thickness of the cloud. The closer the satellite observed SSI is to the estimated clear sky SSI, the less is the contribution from clouds in the DLI estimate.

During daytime, Eq. (14) is used to estimate the cloud contribution coefficients, for night-time conditions, coefficients estimated using Eq. (13) are used. In situ measurements of longwave irradiance have been collocated with NWCSAF PPS cloud type classifications. In this collocation a simplified cloud classification scheme has been used (Table 1). This simplified scheme and the mapping to the NWCSAF PPS cloud types is provided in the column "Code used in DLI". Using this collocation dataset, cloud contribution coefficients for the simplified cloud classifications in Table 1 have been developed. These are reported in Table 2. The stations used in development of the cloud contribution coefficients were Bergen in Norway and Norrköping in Sweden, and a full year of data (2001) was applied.

Further description of choices made in the configuration of the DLI processing is provided in a Technical Report (Godøy, 2004). A schematic representation of the DLI processing chain is provided in Fig. 2. This shows again, as for the SSI product, that the main purpose of the satellite data is to provide a description of the cloud condition.

2.3. Input and validation data

The two algorithms are implemented in an operational processing chain where changes are documented and approved through the framework specified by EUMETSAT using external review teams. The processing chain is fed with locally received AVHRR data in Oslo and data received through EUMETSAT Advanced Retransmission Service (EARS). Data from both NOAA and EUMETSAT satellites are used. The algorithms require additional information on atmospheric water vapour content and surface temperatures. This information was extracted from the local operational NWP model at the Norwegian Meteorological Institute. The model output used in this study was created using HIRLAM (Undén et al., 2002) version 6.4 with a nominal horizontal resolution of approximately 11 km and 60 vertical layers being forced by the ECMWF operational model. At the time when this processing chain was established, this HIRLAM model had better performance along the coast and in the High North according to the operational monitoring performed by the institute. Furthermore, monthly climatological fields of e.g. surface albedo and ozone (collected from TOMS data) are required. Surface albedo over land is adapted for the solar zenith using the approach of Csizsar and Gutman

Table 1
NWC SAF PPS cloud type products and the categorizing of these used in the DLI calculation.

#	Cloud category SAF NWC PPS	Simplified	Code used in DLI
0	Unprocessed	NA	0
1	Cloud free land	Clear	1
2	Cloud free sea		
3	Snow contaminated land		
4	Snow or ice contaminated sea		
5	Very low stratiform cloud	Low clouds	2
6	Very low cumuliform cloud		
7	Low stratiform cloud		
8	Low cumuliform cloud		
9	Medium level stratiform cloud	Medium level clouds	3
10	Medium level cumuliform cloud		
11	High and opaque stratiform cloud	High opaque clouds	4
12	High and opaque cumuliform cloud		
13	Very high and opaque stratiform cloud		
14	Very high and opaque cumuliform cloud		
15	Very thin cirrus cloud	Thin cirrus	5
16	Thin cirrus cloud		
17	Thick cirrus cloud	Thick cirrus	6
18	Cirrus above low or medium level cloud		
19	Fractional or subpixel cloud	Fractional clouds	7
20	Unclassified	NA	0

Table 2
Cloud contribution coefficients developed using collocated satellite and in situ observations at Bergen in Norway and Norrköping in Sweden. These coefficients are generated using a full year (2001) of collocated data.

Class name	C_i
Low clouds	0.7786
Medium level clouds	0.7550
High opaque clouds	0.7262
Thin cirrus	0.6255
Thick cirrus	0.6470
Fractional clouds	0.5751
Clear	0.0000

(1999) over land and Briegleb et al. (1986) over ocean. The AVHRR data used for this study at METNO were processed from HRPT to level 2 using version 6.12 of the EUMETSAT ATOVS and AVHRR Pre-processing Package (AAPP) software which is available from http://nwpsaf.eu/. In flight sensor degradation of visible channels is handled through implementation of updated calibration co-efficients (e.g. Rao and Chen, 1996, 1999). Classification of cloud types have been done using the NWCSAF PPS algorithms and software (NWCSAF, Dybbroe et al., 2005a; 2005b; Karlsson and Dybbroe, 2010).

A map of the available validation datasets for surface radiative stations is provided in Fig. 3. It can readily be seen that validation data is primarily available for Northern Europe. Validation data are received from Norwegian Institute for Agricultural and Environmental Research (only pyranometer measurements covering Norway), University of Bergen, Norway, Finnish Meteorological Institute (FMI), Swedish Meteorological and Hydrological Institute (SMHI), Deutscher Wetterdienst (DWD), UK Meteorological Office (UKMO) and the Norwegian Meteorological Institute. Data from DWD, UKMO and SMHI are available on WMO Global Telecommunication System (GTS), while data from the other sources are received regularly through other mechanisms. A report on which data that are used (Godøy, 2015) is available. In short, few of the GTS observations are used in the current configuration, as they are still in the process of being evaluated. The main problem with using WMO GTS as a data source is that very little information is available on the stations with regards to maintenance frequencies, instrumentation, surroundings, etc. Lacking this information it is hard to determine the quality of the data received. The evaluation of all stations used in this study is based upon visual inspection of time series of data and comparison with results from a Radiative Transfer Model (RTM), libRadtran (Emde et al., 2016), for cloud free conditions. For this purpose version 1.6-beta was used. This comparison with simulated data indicates whether there are shadow effects that should be taken into account for the stations as well. The main intention of the satellite estimates when the development started was to provide information over ocean areas. However, most of the available validation data are located on land. Some of the validation stations have maritime climate conditions (e.g. stations located on islands and on the coast) while others have not (e.g. located in mountainous or forest regions). In order to get sufficient validation data, validation stations without a maritime character have also been included, but the satellite estimates for these locations have been tuned for the local climatological conditions. Following these considerations, a subset (Table 3) of the validation stations available, has been used for routine validation. In this table, stations are identified by names, station identifiers, geographical positions, and which parameters they are employed to validate.

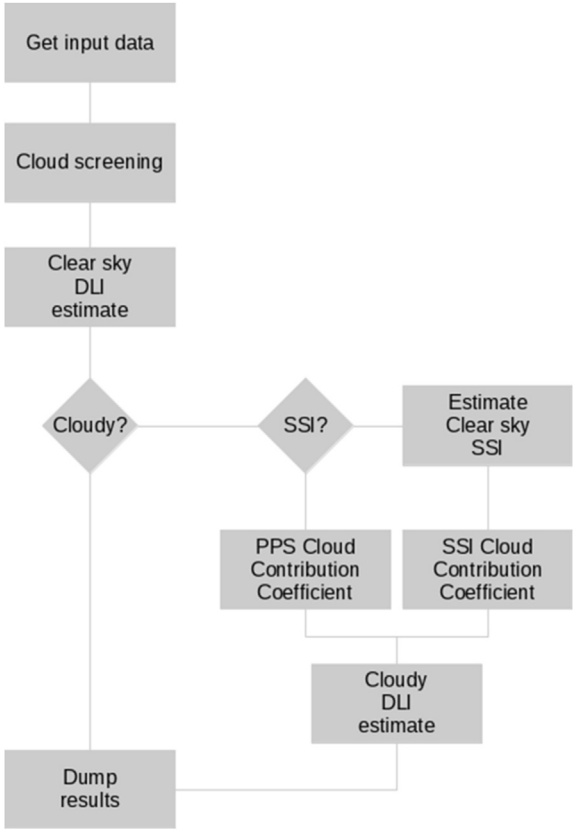

Fig. 2. Same as Fig. 1, but for DLI processing.

3. Results

The operational processing chain produce daily maps of SSI (Fig. 4) and DLI (Fig. 5). These products are provided in a Polar Stereographic map projection with a spatial resolution of 5 km. The product is a daily mean value in Watt per square meter. These products are validated against the in situ observations identified in the previous chapter. The validation process is done on a regular basis with reports to EUMETSAT every 6 months. The validation process starts with an evaluation of all the available in situ data. During this process it is determined whether a specific station shall be used or not. Reasons for excluding a station may be a lack of observations (all or a long period) or changes in the attitude of clear sky observations for solar insolation (e.g. may be caused by construction work or insufficient maintenance). In the examination of the available observations, other deficiencies may also be discovered, leading to observations to be discarded from the validation. When the stations finally have been determined, observational data are aggregated to hourly values (for validation of individual passage products) where this is not done already and subsequently to daily values. Then satellite estimates are collocated with in situ measurements. In this process the number of observations used to establish a daily value as well as the number of satellite passages used in the satellite estimate is recorded. When less than 24 hourly observations are available, the validation of the satellite estimates of daily values is excluded from the analysis reported herein. A similar exclusion of satellite estimates based on the number of passages used for estimating the daily value in a grid cell in the output grid is not done.

Fig. 6 shows the temporal evolution of validation results for SSI for the stations used. The upper panel shows the mean monthly observed insolation in Watt per square meter for all validation stations used in the validation. The seasonal cycle with the winter minimum is quite evident. It is important to remember that in situ

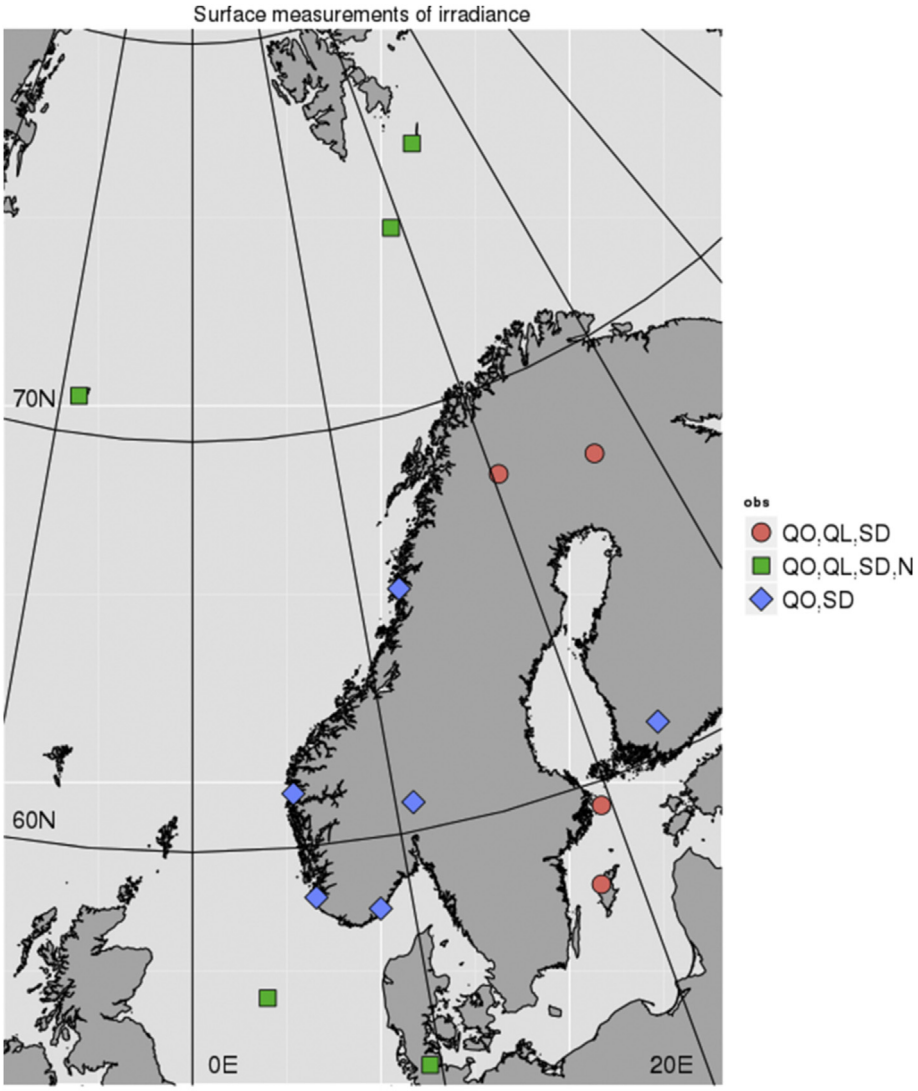

Fig. 3. Map of all available validation stations. The colour legend indicates the types of observations available for each station. QO is SSI, QL is DLI, SD is sunshine duration, and N is cloud cover through manual observation following WMO specifications. (For interpretation of the references to colour in this figure legend, the reader is referred to the web version of this article.)

Table 3
Validation stations currently used for validation of SSI and DLI products from the Ocean and Sea Ice SAF High Latitude Processing Centre.

Station	Id	Lat.	Lon.	Purpose	Status
Apelsvoll	11500	60.70°N	10.87°E	SSI	In use, under examination due to shadow effects.
Landvik	38140	58.33°N	8.52°E	SSI	In use
Særheim	44300	58.78°N	5.68°E	SSI	In use
Fureneset	56420	61.30°N	5.05°E	SSI	In use
Tjøtta	76530	65.83°N	12.43°E	SSI	In use
Ekofisk	76920	56.50°N	3.2°E	SSI, DLI	In use, minor shadow effects at certain directions.
Bjørnøya	99710	74.52°N	19.02°E	SSI, DLI	In use, Arctic station with snow on ground much of the year.
Hopen	99720	76.51°N	25.01°E	SSI, DLI	In use, Arctic station with snow on ground much of the year.
Jan_Mayen	99950	70.93°N	−8.67°E	SSI, DLI	In use, Arctic station with snow on ground much of the year, volcanic ash deteriorates instruments in periods.
Schleswig	10035	54.53°N	9.55°E	SSI, DLI	In use
Hamburg-Fuhlsbuettel	10147	53.63°N	9.99°E	SSI, DLI	In use
Jokioinen	1201	60.81°N	23.501°E	SSI	In use
Sodankylä	7501	67.37°N	26.63°E	SSI, DLI	In use.
Kiruna	02045	67.85°N	20.41°E	SSI, DLI	Only DLI used so far.
Visby	02091	57.68°N	18.35°E	SSI, DLI	Only DLI used so far.
Svenska Högarna	02492	59.45°N	19.51°E	SSI, DLI	Only DLI used so far.

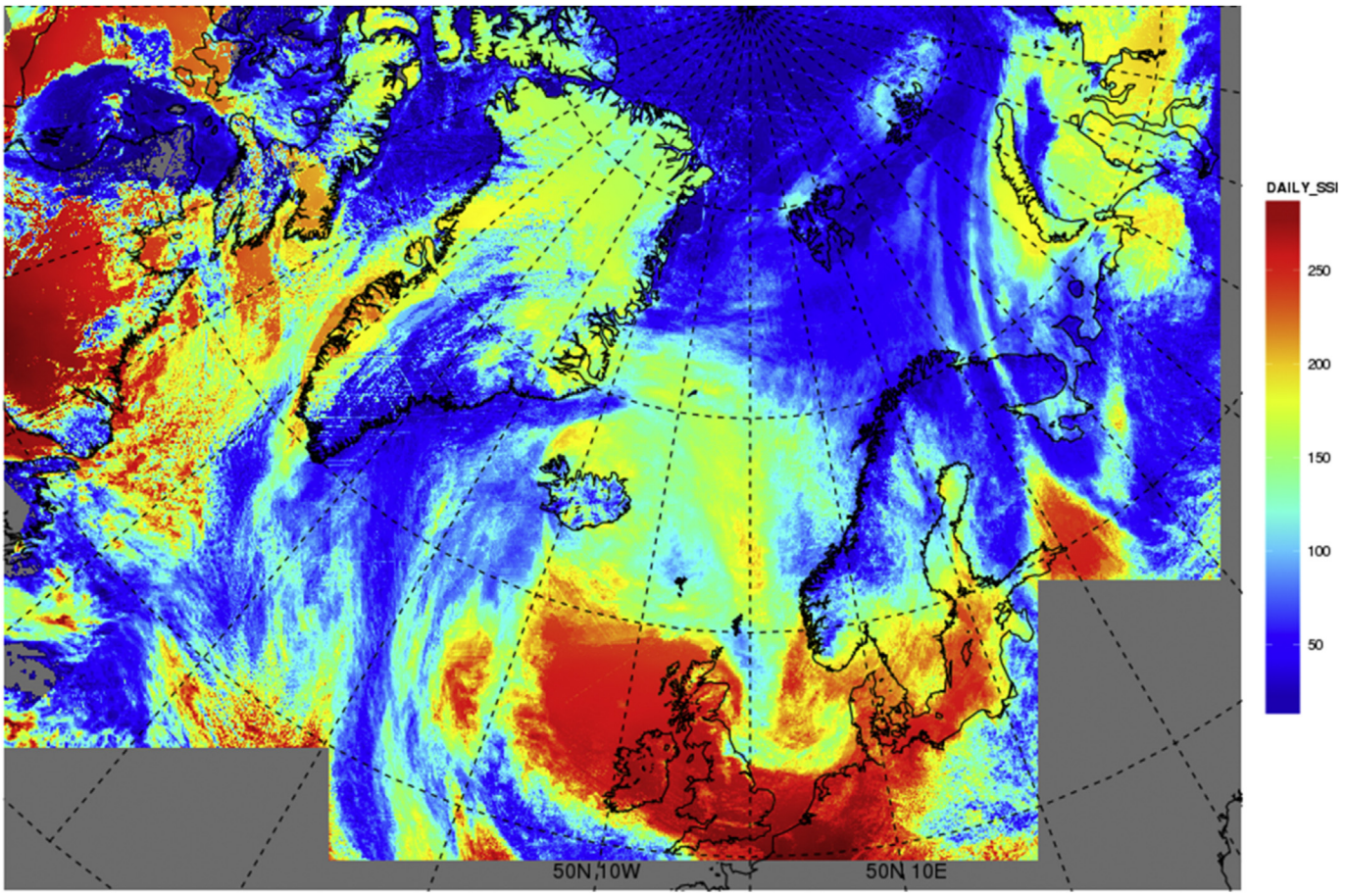

Fig. 4. Daily mean Surface Solar Irradiance as estimated for 2015-04-18.

stations in this study spans latitudes from about 50°N to 74.5°N. Many stations make recordings during winter time with no or very small values of observed insolation. The middle panel shows the difference between the observed and the estimated solar insolation, i.e. the bias with plus/minus one standard error of the monthly mean values presented as a ribbon. The most prominent feature is that the bias is negative in spring and positive in autumn. The negative bias in spring is related to stations with snow cover. The lower panel shows the relative bias, that is the bias (estimated minus observed irradiance) compared to the mean observed insolation. This shows increased values during winter time, but except for this no specific seasonal tendency like the bias. The target requirement for the EUMETSAT Ocean and Sea Ice SAF surface insolation is a relative bias of less than 10%. This is met most of the year for most of the stations, except during winter time and the periods with very low observed insolation when the signal to noise ratio is increased. The correlation coefficient for observed and estimated surface solar irradiance is approximately 0.93. The mean bias for all stations and the full period is −6.0 W/m^2 indicating an underestimation of the SSI. The mean standard deviation of the bias is 17.5 W/m^2.

Fig. 7 shows the temporal evolution of the validation of the DLI for the stations used. The upper panel shows the temporal evolution of the mean monthly observed DLI at the stations used. A seasonal cycle (with large values during summer) is observed but it is less prominent than the cycle found for the SSI. Again it is important to remember that the stations used span several degrees of latitude, thus much variation is embedded in the mean monthly values. The middle panel shows the bias. There is no seasonal cycle evident in this plot, but a slight tendency towards underestimating the DLI. However, this tendency has been reduced since 2014. The lower panel shows the relative bias. This has no evident seasonal cycle either. The target requirement for this product is a relative bias of less than 5%. This requirement is met most of the period, with an exception in the Summer of 2013 and August 2015. The correlation coefficient for observed and estimated downward longwave irradiance is approximately 0.90. The bias is 2.3 W/m^2 and the standard deviation of the bias is 17.7 W/m^2.

4. Discussion

Ohmura et al. (1998) say that the estimated accuracy for BSRN stations measuring shortwave and longwave irradiance at the surface is 5 and 10 W/m^2, respectively. In this study no BSRN stations have been used. The main reason for this was the long delay for data delivery. The stations used in this study is not of BSRN quality, but have a better localisation for validation of the products. It has been attempted to utilise stations with a maritime profile, although this has proven difficult. Among all the stations used, only the station at the oil rig Ekofisk in the North Sea can be classified as a fully maritime station. However, the Arctic stations (Jan Mayen, Bjørnøya and Hopen) as well as many of the stations along the coast of Norway feature a maritime climate. The Arctic stations are located at rather small islands, surrounded by ocean while most of the stations on the Norwegian mainland are located very close to the coast, hence within primarily a maritime atmosphere. The main difference between these stations and purely maritime stations is probably related to the surface albedo. Although most of the

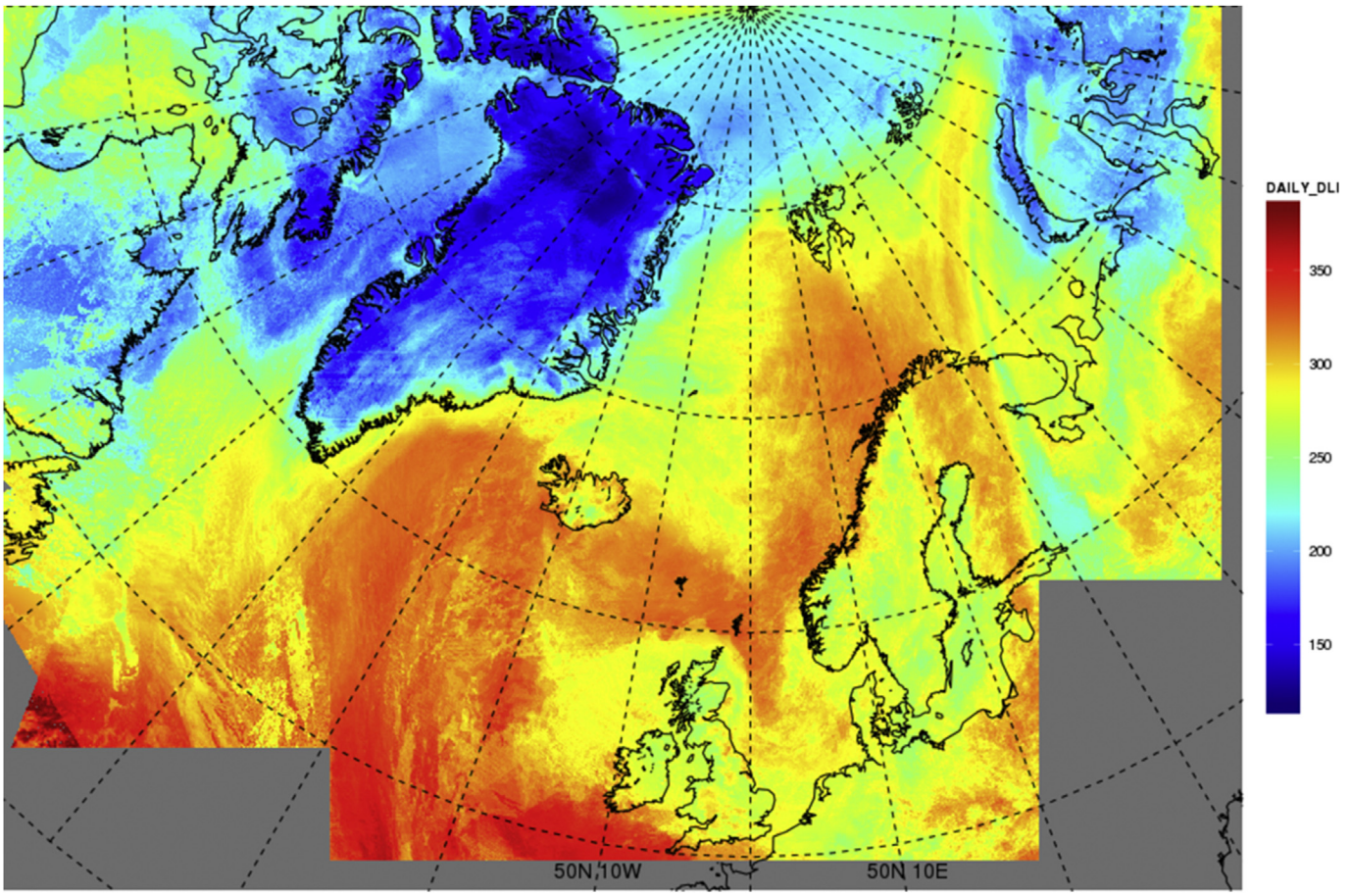

Fig. 5. Same as Fig. 2, but for Downward Longwave Irradiance at the surface.

stations are not experiencing lasting snow cover, and have open water close by, they have a higher surface albedo than purely maritime stations. This is, however, a complicating feature which affects the validation results in a negative manner.

Several of the stations have problems with shadow effects. This is in particular important for the solar irradiance measurements. At Ekofisk, this is caused by masts at the platform. For stations along the Norwegian coast it is caused by the complex topography with high mountains closer to the stations than recommended. This is also the situation at the Arctic stations Jan Mayen and Hopen. For some of the stations that are available through WMO GTS, too little is known about the local topography and they have been excluded for this purpose. The information available for stations and their characteristics will improve drastically when the WMO Integrated Global Observing System (WIGOS) and the WIGOS Operational Information Resource (WIR) become operational. As of today, this information is not easily available. The consequence of this is that most of the stations used in this study have an estimated accuracy that is far less than the assumed 5 and 10 W/m^2 respectively for shortwave and longwave irradiance at the BSRN stations, and this additional error will contribute to the overall uncertainty of the validation results. On a general basis, it is assumed that the shortwave measurements used here are probably slightly lower than the real solar irradiance. The reason for this is that several of the stations have issues with shadow effects. For some stations where the shadow effects have been well analysed and understood, correction formulas have been developed. For some stations, the analysis of shadow effects resulted in removal of the station from the validation effort. Many of the remaining stations have limited shadow effects, as it is very hard to find observations in this region that is unaffected by the complex topography, but these effects have been considered to be acceptable for this study. The evaluation of shadow effects have been based on photography of the surroundings where that has been available combined with comparison of cloud free observations with RTM simulations for clear sky. Observed and estimated daily curves of solar insolation for various periods of the year have been compared and used to create correction factors at stations where a sufficient number of clear sky situations have been found. The number of clear sky situations available throughout the year to create such correction factors is however very limited in this geographical area.

Concerning the SSI product, this study showed a bias of −6.0 and standard deviation of 17.5 W/m^2. However, the issues contributing to the bias are varying. On a general basis it is observed that satellite estimates are overestimating the solar insolation at high latitudes (in the Barents and Greenland Seas) and underestimating it in other areas. The underestimation is most prominent on stations along the Norwegian Coast and in Spring. This coincides with snow covered surfaces and frequent scattered clouds, features supporting over-irradiance (Yordanov et al., 2013). This feature is not at all captured by satellite data and may be a contribution to the underestimation. How large this contribution potentially is, is not known nor has it been examined in detail so far. The reason for the overestimation of SSI in the Barents and Greenland Seas is not fully understood. Potential explanations are related to the tuning of algorithms with respect to aerosol loads and usage of climatological fields for ozone, but the far most important issue affecting the quality of the SSI products is the quality of the cloud type information gained from

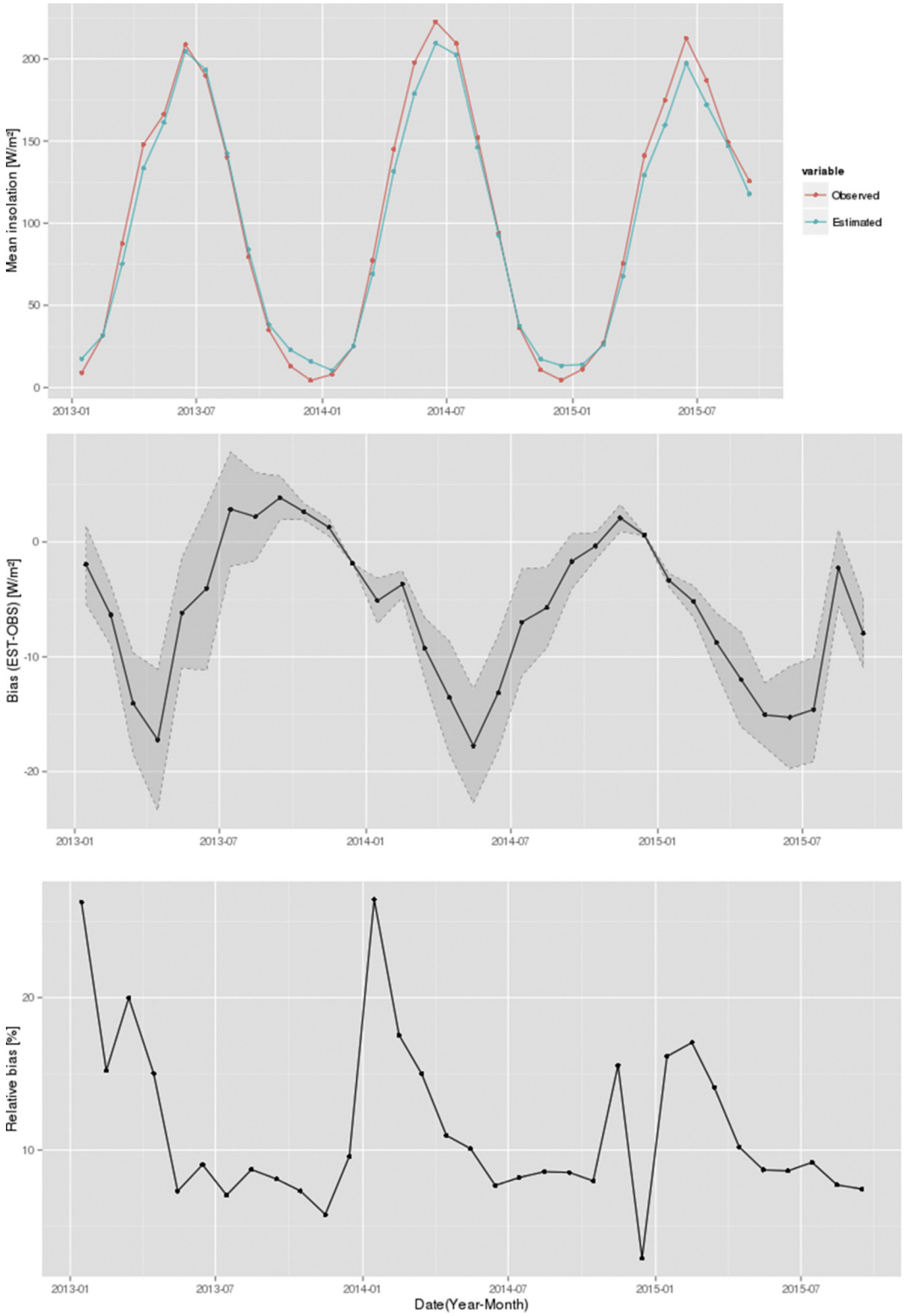

Fig. 6. Time series of monthly mean observed insolation (upper panel), bias (middle panel) and relative bias (lower panel) for the stations under evaluation. In the middle panel plus/minus one standard error for the monthly mean is indicated by the ribbon.

the NWCSAF Polar Platform System (PPS) software (Dybbroe et al., 2005a, 2005b; Karlsson and Dybbroe, 2010). To illustrate this, the following examination of observations is useful. June 12, 2014 was a day with almost no clouds at Jan Mayen. The following day, June 13 was quite cloudy. The difference in the observed daily irradiance between these two days was almost 200 W/m^2. A preliminary study of the PPS quality was performed in 2004, using data for the period February 11, 2003 through June 9, 2004. In that study synoptic observations of the cloud cover at Norwegian weather stations and type was compared with PPS results (version 0.3.0 at that

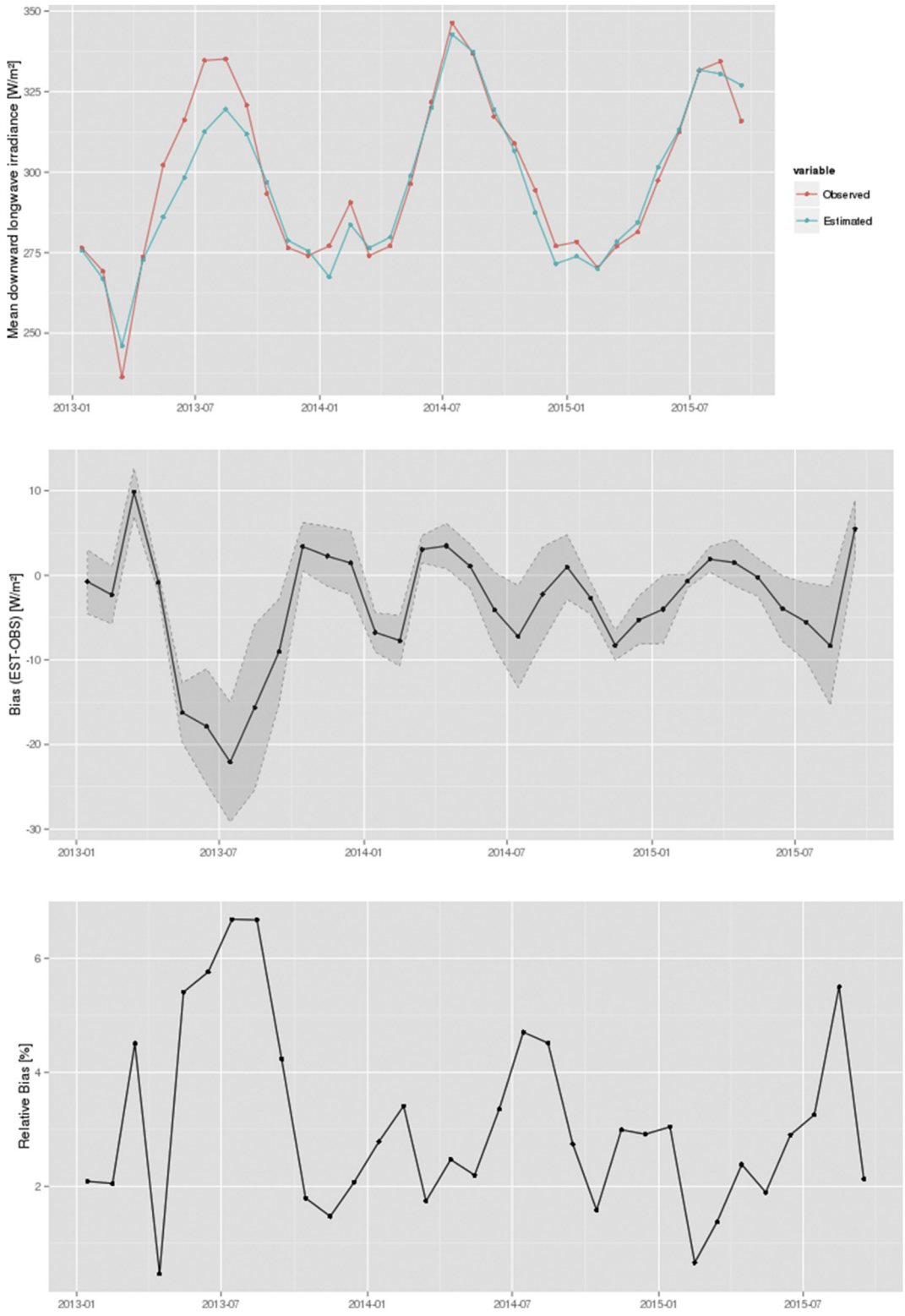

Fig. 7. Same as Fig. 4, but for longwave irradiance.

time). The study showed that PPS had a tendency to tag cloudy pixels as clear and that this tendency was most pronounced in cases of low and medium height clouds. PPS has evolved much since that, but some of the issues remain. The quality of PPS in Polar regions was more thoroughly examined by Karlsson and Dybbroe (2010) through comparison with Calipso-Caliop data. They found that while the cloud amount was fairly accurate, it was challenging to determine the cloud types during the Polar Summer. They found that PPS generally underestimated the fractional cloud cover and that many low clouds goes undetected. This can explain part of the overestimation of SSI, but further examination of the performance of the PPS products at High Latitudes is required. Such an

evaluation should be done using in situ measurements of cloud cover and type at the stations where SSI are evaluated.

In general, the results are slightly poorer than the results achieved for the Climate Monitoring SAF (CMSAF) data against BSRN validation data (Posselt et al., 2012) for daily data. However, there are some major differences. The CMSAF results are based on geostationary data which are received several times every hour while the OSISAF High Latitude (HL) products are based on polar orbiting satellites with irregular temporal coverage throughout the day. Furthermore, this study is not based on BSRN station data, but on in situ observations of lesser quality. In that perspective, the results are comparable. The irregular temporal coverage of near sun-synchronous polar orbiting satellites throughout the day creates problems concerning proper description of the atmospheric conditions throughout the day. Although polar orbiting satellites have a return period of approximately 100 min, the near sun-synchronous properties create a highly variable observation geometry for the target areas. This variation in the observation geometry affects the results since e.g. anisotropy corrections are rather poorly described for some surfaces under consideration. Using geostationary satellites, there is a new observation of a target area every 15 min. The illumination conditions change, but the observation geometry is rather stable compared with polar orbiting satellites. The number of available observations from polar orbiting satellites is far less. Acknowledging how variable the cloud cover is as well as the diurnal cycle of the solar insolation, this creates problems when estimating the daily mean insolation. These problems do affect the overall performance of the products, but still results are comparable to results achieved at lower latitudes using geostationary satellite data as input (Posselt et al., 2012). Posselt et al. (2012) did also evaluate the monthly values for the CMSAF, while Ineichen et al. (2009) evaluated and compared the hourly values for CMSAF, Land SAF and OSISAF. Such a comparison is not performed herein.

Concerning the DLI product, this study showed a bias of 2.3 W/m^2 and a standard deviation of the bias of 17.7 W/m^2. Target requirements were met most of the period and there were no obvious issues found as for the SSI estimates. However, there is a slight tendency towards underestimation of the DLI in the Barents and Greenland Seas. This is consistent with the overestimation of the SSI in the same region. This overestimation of SSI is related to issues with the performance of the PPS cloud cover and cloud types (Karlsson and Dybbroe, 2010) as discussed above. A methodological problem that is not addressed by upgrading the PPS software is the fact that cloud bottom height has strong influence on the DLI products. However, using optical satellite data to describe cloud properties, clouds are described through the appearance of the cloud top (as seen from the satellite) rather than the cloud bottom. Properties of clouds (e.g. optical thickness and height) are reflected in the cloud factor through statistical representation of clouds at the validation stations for night time conditions or using the SSI during daytime. This observation geometry is a constraint of the methodology. It affects the quality of the results, and it is difficult to circumvent this constraint with the currently available input data. The cloud contribution coefficients used in this study were developed on a limited number of in situ stations using an old version of the PPS. Still, the DLI estimates perform well when compared with a wide range of in validation stations. It is, however, time to redo the collocation of PPS cloud types and in situ measurements of longwave irradiance on the surface to get updated cloud contribution coefficients. In situ measurements in the Arctic are now available. This was not the situation when the first coefficients were estimated and it will allow a geographical separation of results if needed.

An important issue using near sun-synchronous satellites for estimation of daily values is that temporal coverage is good some times during the day while other periods are lacking information. This issue has proven to have the largest impact on the SSI product, leaving the DLI product slightly less affected. Most people have experienced the immediate and direct effect of clouds on sunshine. Under conditions with broken cloud cover, the experienced insolation by an observer at the ground may change rapidly. This rapid change in insolation is well covered by in situ measurements which normally provides measurements that are aggregated at 1 min, 10 min or hourly intervals. The polar orbiting satellite on the other hand, does not cover this rapid change in cloud cover and subsequent insolation. Another complicating issue when working with SSI and DLI over oceans and in Polar regions is the availability of validation data. In this study, all validation stations except one is located onshore. Offshore observations are expensive and difficult to maintain over time. The only exception is the Ekofisk station located on an oil rig in the North Sea. Unfortunately, this station is currently non-operational due to a replacement of the oil rig on which it has been mounted. The equipment has been rescued and work is in progress to mount it on the new platform. However, mounting equipment on oil rigs is not a straightforward task provided the strict regulations connected to the operating environment. Fortunately, the validation of OSISAF radiative fluxes have been very good throughout the period when information from these instruments have been available.

5. Conclusions

More than 2.5 years of SSI and DLI estimates using satellite data have been validated against in situ measurements. This evaluation has identified challenges concerning the availability of suitable surface measurements of radiative fluxes for validation purposes. These challenges include the influence of the complex topography of the region on measurements, but also the availability of sustained observations over ocean and sea ice. Sustained observations are required to properly validate operational products, especially in a quantitative manner. During validation, issues related to the quality of the validation data as well as algorithm input data and tuning have been identified. Furthermore, issues related to incorrect cloud mask and cloud type input data have been identified. It is observed that the performance of the SSI validation is poorer over sea ice or snow covered surfaces at high latitudes. The reason for this is not fully understood. It can be related to the snow cover itself, but also to a seasonal dependency in aerosol optical depth (Augustin Mortier, personal communication). Finally, the current system configuration utilise climatological values for some input data while there are dynamic sources available at least for some of the variables in question. These issues will be further examined and a new processing scheme is under development.

Information from the Polar regions, and in particular over the sea ice, has been identified as a gap in the evaluation of these products. In 2014/2015, Professor Yngve Kristoffersen and Audun Tholfsen established the FRAM 2014/2015 ice drift station. The main purpose was to monitor the geological and oceanographic conditions in the Arctic Ocean, but they also performed atmospheric measurements. Among these were measurements of the surface radiative fluxes. These data are now quality controlled and in the process of collocation with satellite data for further analysis of the SSI and DLI quality over sea ice. The availability of new validation datasets will improve the knowledge of the quality of the satellite estimated surface irradiances over sea ice. Furthermore, data from BSRN stations are now available faster than earlier and validation against BSRN stations at Lerwick, Ny-Ålesund, and Toravere is planned.

The current processing setup use information from a local version of the HIRLAM model at the Norwegian Meteorological

Institute. Due to an extension of the area of interest, the NWP input will switch to ECMWF in the future.

Acknowledgement

The production system for surface radiative fluxes was implemented, tested and operated with support from EUMETSAT. In situ observations at the Arctic stations Bjørnøya, Jan Mayen, and Hopen has been supported by the Research Council of Norway through IPY projects IPY-THORPEX (175992/S30) and iAOOS-Norway (176096/S30). The author would also like to thank the anonymous reviewers for very valuable comments in the review process.

References

Briegleb, B.P., Minnis, P., Ramanathan, V., Harrison, E., 1986. Comparison of regional clear-sky albedos inferred from satellite observations and model computations. J. Clim. Appl. Meteorol. 25, 214–226.

Brisson, A., Le Borgne, P., Marsouin, A., Moreau, T., 1994. Surface irradiances calculated from Meteosat sensor data during SOFIA-ASTEX. Int. J. Rem. Sens. 15 (1), 197–203.

Brisson, A., LeBorgne, P., Marsouin, A., 1999. Development of Algorithms for Surface Solar Irradiance Retrieval at O&SI SAF Low and Mid Latitudes. Internal report at Météo France/SCEM/CMS, 22302 Lannion, France, February 1999.

Brisson, A., Le Borgne, P., Marsouin, A., 2000. Development of Algorithms for Downward Longwave Irradiance Retrieval at O&SI SAF Low and Mid Latitudes. Project Report O&SI SAF Low and Mid Latitudes, Meteo-France/SCEM/CMS/, 22302 Lannion, France, February 2000.

Csizsar, I., Gutman, G., 1999. Mapping global land surface albedo from NOAA AVHRR. J. Geophys. Res. 104 (D6), 6215–6228.

Darnell, W.L., Staylor, F., Gupta, S.K., Denn, F.M., 1988. Estimation of surface insolation using sun-synchronous satellite data. J. Clim. 1, 820–835.

Darnell, W.L., Staylor, W.F., Gupta, S.K., Ritchey, N.A., Wilbur, A.C., 1992. Seasonal variation of surface radiation budget derived from international satellite cloud climatology project C1 data. J. Geophys. Res. 97, 15 741–15 760.

Dybbroe, A., Karlsson, K.-G., Thoss, A., 2005a. NWCSAF AVHRR cloud detection and analysis using dynamic thresholds and radiative modelling - Part I: algoritm description. J. Appl. Meteor. 44, 39–54.

Dybbroe, A., Karlsson, K.-G., Thoss, A., 2005b. NWCSAF AVHRR cloud detection and analysis using dynamic thresholds and radiative modelling - Part II: tuning and validation. J. Appl. Meteor. 44, 55–71.

Emde, C., Buras-Schnell, R., Kylling, A., Mayer, B., Gasteiger, J., Hamann, U., Kylling, J., Richter, B., Pause, C., Dowling, T., Bugliaro, L., 2016. The libRadtran software package for radiative transfer calculations (version 2.0.1). Geosci. Model Dev. 9, 1647–1672. http://dx.doi.org/10.5194/gmd-9-1647-2016.

Frouin, R., Chertock, B., 1992. A technique for global monitoring of net solar irradiance at the Ocean surface. Part I: model. J. Appl. Met. 31, 1056–1066.

Godøy, Ø., 2000. Evaluation of Clear Sky Solar Irradiance Algorithms at High Latitudes. DNMI Research Note No. 36. ISSN: 0332-9879. Norwegian Meteorological Institute, Oslo, Norway, 2002, 13pp.

Godøy, Ø., Eastwood, S., 2002a. Testing of Short-wave Irradiance Retrieval Algorithms under Cloudy Conditions. DNMI Research Note No. 69. ISSN: 0332-9879. Norwegian Meteorological Institute, Oslo, Norway, 2002, 20pp.

Godøy, Ø., Eastwood, S., 2002b. Narrowband to Broadband Correction of NOAA/AVHRR Data. DNMI Research Note No. 69. ISSN: 0332-9879. Norwegian Meteorological Institute, Oslo, Norway, 2002, 12pp.

Godøy, Ø., Eastwood, S., 2002c. Preliminary Validation Results of Ocean and Sea Ice SAF HL Short-wave Irradiance Estimates Using AVHRR Data. DNMI Research Note No. 70. ISSN: 0332-9879. Norwegian Meteorological Institute, Oslo, Norway, 2002, 21pp.

Godøy, Ø., 2004. Tuning and Validation of a Downward Longwave Irradiance Retrieval Algorithm. Research Note No. 02/04 Remote Sensing. ISSN: 1503-8009. Norwegian Meteorological Institute, Oslo, Norway, 2004, 12pp.

Godøy, Ø., 2015. Validation Data for Surface Radiative Fluxes. OSISAF Technical Report, 2015 (accessed 09.10.2016). http://osisaf.met.no/docs/osisaf_cdop2_ss2_rep_flux-val-data_v1p0.pdf.

Goff, J.A., Gratch, S., 1946. Low-pressure properties of water from -160 to 212 F. Trans. Am. Soc. Heat. Vent. Eng. 52, 95–121.

Hucek, R., Jacobowitz, H., 1995. Impact of scene dependence on AVHRR albedo models. J. Atm. Oce. Tech. 12 (4), 697–711.

Ineichen, P., Barroso, C.S., Geiger, B., Hollmann, R., Marsouin, A., Mueller, R., 2009. Satellite application facilities irradiance products: hourly time step comparison and validation over Europe. Int. J. Remote Sens. 30, 5549–5571.

Karlsson, K.-G., Dybbroe, A., 2010. Evaluation of arctic cloud products from the EUMETSAT climate monitoring satellite application facility based on CALIPSO-CALIOP observations. Atmos. Chem. Phys. 10, 1789–1807. http://dx.doi.org/10.5194/acp-10-1789-2010.

List, R.J., 1984. Smithsonian Meteorological Tables. Smithsonian Institution Press, Washington, USA.

Manalo-Smith, N., Smith, G.L., Tiwari, S.N., Staylor, W.F., 1998. Analytic forms of bidirectional reflectance functions for application to Earth radiation budget studies. J. Geophys. Res. 103 (D16), 19 733–19 751.

Ohmura, A., Dutton, E.G., Forgan, B., Fröhlich, C., Gilgen, H., Hegner, H., Heimo, A., König-Langlo, G., McArthur, B., Müller, G., Philipona, R., Pinker, R., Whitlock, C.H., Dehne, K., Wilda, M., 1998. Baseline surface radiation network (BSRN/WCRP): new precision radiometry for climate research. Bull. Am. Meteorol. Soc. 79 (10), 2115–2136.

Paltridge, G.W., Platt, C.M.R., 1976. Radiative Processes in Meteorology and Climatology. Elsevier, ISBN 0-444-41444-4.

Prata, A.J., 1996. A new long-wave formula for estimating downward clear-sky radiation at the surface. Q.J.R. Meteorol. Soc. 122 (533), 1127–1151.

Posselt, R., Mueller, R.W., Stöckli, R., Trentmann, J., 2012. Remote sensing of solar surface radiation for climate monitoring — the CM-SAF retrieval in international comparison. Remote Sens. Environ. 118, 186–198. http://dx.doi.org/10.1016/j.rse.2011.11.016.

Rao, C.N.R., Chen, J., 1996. Post-launch calibration of the visible and near-infrared channels of the advanced very high resolution radiometer on the NOAA-14 spacecraft. Int. J. Rem. Sens. 17, 2743–2747.

Rao, C.R.N., Chen, J., 1999. Revised post-launch calibration of the visible and near-infrared channels of the Advanced Very High Resolution Radiometer (AVHRR) on the NOAA-14 spacecraft. Int. J. Rem. Sens. 20 (18), 3485–3491.

Undén, P., et al., 2002. HIRLAM-5 Scientific Documentation, HIRLAM-5 Project. SMHI Tech. Rep., 146 pp. [Available from: SMHI, Folkborgsvagen 1, S-60176 Norrköping, Sweden].

Yordanov, G.H., Midtgård, O.-M., Saetre, T.O., Kofoed Nielsen, H., Norum, L.E., 2013. Overirradiance (cloud enhancement) events at high latitudes. IEEE J. Photov. 3 (1), 271–277. http://dx.doi.org/10.1109/JPHOTOV.2012.2213581.